

Mediator proteins orchestrate enzyme-ssDNA assembly during T4 recombination-dependent DNA replication and repair

Jill S. Bleuit, Hang Xu, Yujie Ma, Tongsheng Wang, Jie Liu, and Scott W. Morrical*

Department of Biochemistry, University of Vermont College of Medicine, Burlington, VT 05405

Studies of recombination-dependent replication (RDR) in the T4 system have revealed the critical roles played by mediator proteins in the timely and productive loading of specific enzymes onto single-stranded DNA (ssDNA) during phage RDR processes. The T4 recombination mediator protein, *uvsY*, is necessary for the proper assembly of the T4 presynaptic filament (*uvsX* recombinase cooperatively bound to ssDNA), leading to the recombination-primed initiation of leading strand DNA synthesis. In the lagging strand synthesis component of RDR, replication mediator protein *gp59* is required for the assembly of *gp41*, the DNA helicase component of the T4 primosome, onto lagging strand ssDNA. Together, *uvsY* and *gp59* mediate the productive coupling of homologous recombination events to the initiation of T4 RDR. *UvsY* promotes presynaptic filament formation on 3' ssDNA-tailed chromosomes, the physiological primers for T4 RDR, and recent results suggest that *uvsY* also may serve as a coupling factor between presynapsis and the nucleolytic resection of double-stranded DNA ends. Other results indicate that *uvsY* stabilizes *uvsX* bound to the invading strand, effectively preventing primosome assembly there. Instead, *gp59* directs primosome assembly to the displaced strand of the D loop/replication fork. This partitioning mechanism enforced by the T4 recombination/replication mediator proteins guards against antirecombination activity of the helicase component and ensures that recombination intermediates formed by *uvsX/uvsY* will efficiently be converted into semiconservative DNA replication forks. Although the major mode of T4 RDR is semiconservative, we present biochemical evidence that a conservative "bubble migration" mode of RDR could play a role in lesion bypass by the T4 replication machinery.

Bacteriophage T4 provides an excellent model system for biochemical and genetic studies of recombination-dependent replication (RDR), because DNA replication and recombination are closely coupled throughout much of the phage life cycle. After infecting a host *Escherichia coli* cell, T4 first replicates its genome via an origin-dependent replication initiation pathway. This pathway is shut off after a few rounds of replication, after expression of the T4 *uvsW* RNA/DNA helicase, which resolves R loops required for origin function (1). T4 then relies on a recombination-dependent mechanism to initiate DNA synthesis, and this pathway accounts for a large fraction of the total DNA synthesis observed during T4 infection. In the T4 RDR pathway (reviewed in refs. 2 and 3), branched recombination intermediates generated by the phage homologous recombination machinery are captured and converted into semiconservative DNA replication forks. T4 RDR requires all of the major phage-encoded DNA replication and recombination enzymes including: *gp43* (DNA polymerase), *gp45* (sliding clamp), *gp44/62* (clamp loader), *gp32* [single-stranded DNA (ssDNA) binding protein or *ssb*], *gp61* (primase), *gp41* (DNA helicase), *gp59* (helicase loader; replication mediator protein or RMP),

uvsX (general recombinase), *uvsY* (recombination mediator protein or RMP), and *gp46/47* (recombination exonuclease).

T4 RDR *in Vitro*: Mechanisms and Questions

Work in the Bruce Alberts laboratory led to the reconstitution of a purified *in vitro* system that reproduces major elements of T4 RDR (refs. 4 and 5; J. Barry, M. L. Wong, and B. Alberts, personal communication). Fig. 1 shows the enzymatic steps in the T4 RDR *in vitro* reaction. The priming event that initiates the leading strand synthesis component of RDR is catalyzed by the T4 RecA homolog, *uvsX* protein. *UvsX* forms a presynaptic filament on a ssDNA "primer," which, during T4 infection, usually consists of a 3' ssDNA tail formed during origin-dependent replication of the phage linear duplex. Formosa and Alberts (4), using a linear piece of ssDNA in place of the tailed primer, found that *uvsX* catalyzes the invasion of the ssDNA 3' end into a homologous duplex. Under physiological conditions, this reaction also requires the T4 *uvsY* and *gp32* proteins; their roles in recombination are described below. The resulting D-loop structure contains a primed template capable of initiating DNA synthesis by the T4 DNA polymerase holoenzyme. Addition of holoenzyme plus either of two T4 DNA helicases (*dda* or *gp41/gp59*) results in extensive leading strand DNA synthesis, initially by a conservative, "bubble migration" mechanism. The initiation of lagging strand synthesis reconstitutes a standard semiconservative replication fork, leading to the cessation of bubble migration synthesis. Lagging strand synthesis in the RDR *in vitro* system requires not only the phage primosome (*gp41* helicase + *gp61* primase), but an additional factor as well: the *gp59* protein, which we describe in detail below. The strict requirement for *gp59* to reconstitute lagging strand synthesis in the RDR *in vitro* reaction mirrors the dependence of RDR processes on *gp59 in vivo*.

Biochemical studies of T4 RDR made possible by this *in vitro* system have revealed some of the key mechanistic features of the RDR pathway (refs. 4 and 5; J. Barry, M. L. Wong, and B. Alberts, personal communication). First is the strict requirement, under physiological conditions, for an RMP protein (*uvsY*) to promote the *uvsX*-catalyzed initiation of leading strand synthesis via the D loop-forming mechanism mentioned above. Second is the requirement for another mediator protein (*gp59*) to initiate the lagging strand synthesis component of

This paper results from the National Academy of Sciences colloquium, "Links Between Recombination and Replication: Vital Roles of Recombination," held November 10–12, 2000, in Irvine, CA.

Abbreviations: RDR, recombination-dependent replication; ssDNA, single-stranded DNA; dsDNA, double-stranded DNA; RMP, recombination/replication mediator protein; DSb, DNA double-strand break.

*To whom reprint requests should be addressed at: Department of Biochemistry, University of Vermont College of Medicine, B411A Given Building, Burlington, VT 05405. E-mail: smorrica@zoo.uvm.edu.

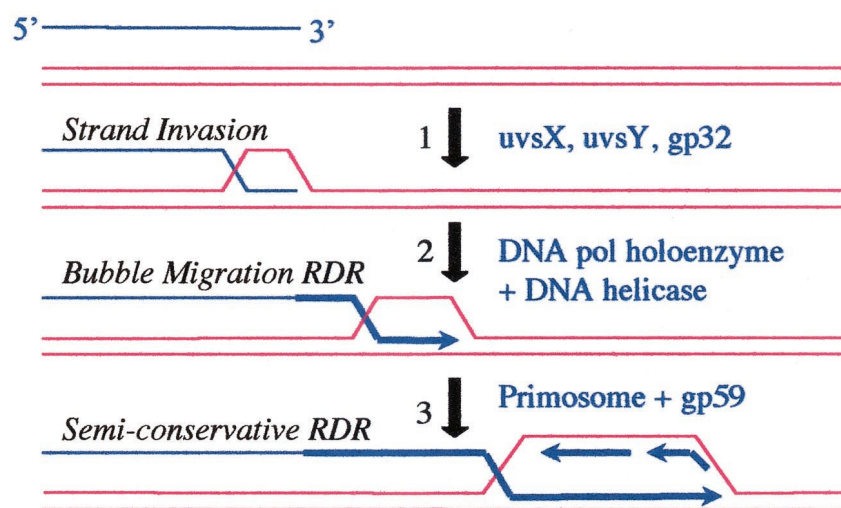


Fig. 1. T4 *in vitro* system for RDR. Step 1: The 3' end of linear ssDNA primer (blue) invades homologous dsDNA template (red) in reaction catalyzed by uvsX recombinase and stimulated by uvsY and gp32. Step 2: DNA polymerase holoenzyme uses primer terminus in D loop to initiate leading strand synthesis. Reaction requires a functional T4 DNA helicase (either dda or gp41/gp59). Branch migration of the trailing junction displaces the daughter strand from the template, leading to conservative (a.k.a. bubble migration) DNA synthesis. Step 3: Strand-specific assembly of functional primosome (gp41 helicase/gp61 primase) on displaced strand of D loop, a reaction requiring gp59. Lagging strand synthesis within the "bubble" reconstitutes a semiconservative replication fork, freezes branch migration and halts bubble migration synthesis.

RDR. Third is the intriguing observation, diagrammed in Fig. 1, that the synthesis of Okazaki fragments always occurs on the displaced strand of the D loop, and not on the 5' extension of the invading ssDNA. The latter point indicates that primosome loading must be strand-specific within the T4 RDR enzymatic machinery, implying that spatial and temporal partitioning of enzyme-DNA assembly processes must occur. The mechanism of strand-specific primosome assembly during T4 RDR is the major focus of this article. Evidence indicates that mediator proteins gp59 and uvsY both play critical roles in maintaining the proper partitioning of where enzyme-DNA complexes are assembled, therefore we begin with a review of the biochemical properties of these RMPs and their specific roles in T4 RDR processes.

Role of UvsY Protein in Assembly of the T4 Presynaptic Filament

The T4 uvsY protein mediates homologous recombination by promoting the assembly of uvsX-ssDNA presynaptic filaments. The biochemical properties of uvsY include the following: At physiological salt concentrations, uvsY protein exists predominantly as a hexamer of identical 15.8-kDa subunits (6). Interestingly the uvsX protein also appears to exist as a hexamer in solution (J.L. and S.W.M., unpublished results). UvsY binds tightly but noncooperatively to ssDNA (7) and has weaker affinity for double-stranded DNA (dsDNA). It exhibits specific protein-protein interactions with other T4 recombination proteins including uvsX, gp32, and gp46/47 (ref. 8; Table 1). UvsY stimulates the DNA strand exchange activity of uvsX protein and is essential for uvsX activity at elevated concentrations of salt and/or gp32, conditions that approximate the physiological situation encountered by the T4 recombination system *in vivo* (8–11). The latter observation explains the apparent codependence of T4 RDR processes on wild-type *uvsX* and *uvsY* gene function *in vivo*. In the T4 RDR *in vitro* system, uvsY dramatically lowers the critical concentration of uvsX protein required for initiating the leading strand synthesis component (5). UvsY carries out two important functions that enable it to stimulate uvsX-catalyzed recombination events (9, 12): (i) uvsY helps uvsX displace gp32 from ssDNA, a reaction necessary for proper formation of the presynaptic filament; and (ii) uvsY

interacts with and stabilizes uvsX-ssDNA filaments after they are assembled.

To catalyze the strand invasion event that initiates RDR, the uvsX recombinase must first form a presynaptic filament on the primer strand. To do so, uvsX must displace gp32, a protein with much higher affinity for the ssDNA. UvsY plays a critical role in promoting this displacement reaction (Fig. 2A). Due to its abundance, high affinity, and cooperativity, gp32 rapidly saturates all ssDNA generated during T4 infection. Nucleating uvsX-ssDNA filament assembly on a preexisting gp32-ssDNA complex is a kinetically slow and thermodynamically unfavorable reaction. UvsY appears to lower this kinetic and thermodynamic barrier to presynapsis by modifying the structure of ssDNA within gp32-ssDNA complexes in a way that favors displacement of gp32 by uvsX protein (12). Within a tripartite uvsY-gp32-ssDNA complex, gp32-ssDNA interactions are destabilized as evidenced by their increased sensitivity to disruption by salt. The destabilization of gp32-ssDNA interactions is postulated to arise through a disruption of gp32 neighbor-neighbor cooperative interactions, perhaps caused by a wrapping of the ssDNA around a uvsY hexamer (Fig. 2A). Disruption of gp32's cooperativity

Table 1. Protein affinity chromatography of T4 Gp46, Gp47, and UvsY

	Eluting protein		
	gp46	gp47	uvsY
gp46-agarose	ND	ND	0.2 M
gp47-agarose	0.6 M	ND	0.2–0.6 M
uvsY-agarose	0.2–0.6 M	0.2–2.0 M	ND
BSA-agarose	FT	FT	FT

Details of the expression, purification, and characterization of T4 gp46 and gp47 proteins will be published elsewhere. Gp46 and gp47 protein bind to each other and to the uvsY protein. NaCl concentrations required for elution of various protein species from indicated affinity column are listed. FT denotes elutes in flow-through (buffer with 0.05 M NaCl). ND denotes not determined. Protein affinity columns were made and chromatography experiments were conducted as described (21). Column running buffer contained 20 mM Tris-HCl (pH 8.1), 1 mM EDTA, 5 mM 2-mercaptoethanol, 5 mM magnesium chloride, and 10% (wt/vol) glycerol, plus either 0.05, 0.2, 0.6, or 2.0 M NaCl in successive elution steps with all other buffer components being identical.

Table 2. Assay for exonuclease activity of Gp46 +/- Gp47

Protein	Label	% Label retained
Substrate = uniformly ^{32}P -labeled linear dsDNA		
None (ctrl)	Uniform	100
gp47	Uniform	100
gp46	Uniform	44
gp46 + gp47	Uniform	14
Substrate = 5' or 3' ^{32}P -labeled linear dsDNA		
gp46	3'	96
gp46	5'	38

Gp46 is a 5' \rightarrow 3' exonuclease and is stimulated by gp47. Either 20 $\mu\text{g}/\text{ml}$ gp46 alone, 20 $\mu\text{g}/\text{ml}$ gp47 alone, or 20 $\mu\text{g}/\text{ml}$ gp46 + 20 $\mu\text{g}/\text{ml}$ gp47 was incubated with 20 μM (nucleotides) of a PCR-generated blunt-ended 0.9-kb dsDNA fragment uniformly labeled with α - ^{32}P -dTTP. Reaction buffer contained 20 mM Tris-acetate (pH 7.4), 10 mM magnesium acetate, and 90 mM potassium acetate. Constant salt conditions were maintained by adding protein storage buffers to reactions in appropriate amounts. Reactions (45 μl) were incubated at 37°C, and a 10- μl aliquot was removed at $t = 5$ min and tested for acid-insoluble counts as described (4). For 5' or 3' ^{32}P -labeled linear dsDNA, reactions contained 2 $\mu\text{g}/\text{ml}$ gp46 and DNA consisting of *EcoRI*-linearized M13mp19 dsDNA labeled with ^{32}P at either its 3' or 5' end by using standard methods.

would greatly increase the probability of uvsX protein locally displacing gp32 to nucleate presynaptic filament formation (12, 13).

Stabilization of uvsX-ssDNA presynaptic filaments is another important function of uvsY (9). UvsX-ssDNA filaments are markedly more resistant to disruption by elevated salt concentrations in the presence of uvsY than in its absence. This effect appears to require direct interactions between uvsY and uvsX. Evidence suggests that uvsY significantly slows the dissociation of uvsX from ssDNA that normally occurs after ATP hydrolysis

by the recombinase. As a consequence, uvsX-catalyzed DNA branch migration, believed to be coupled to its ATPase-driven ssDNA association/dissociation cycle, is inhibited by uvsY (14). Thus uvsY paradoxically stimulates the presynapsis and synapsis phases of homologous recombination while inhibiting the branch migration phase. It has been proposed that this inhibition necessitates the action of a DNA helicase to complete branch migration (14). A further consequence of uvsY's stabilization of uvsX-ssDNA is that it effectively sequesters ssDNA in the filament from replication proteins that must interact with ssDNA for their function. This issue will be explored in a later section.

The stoichiometry of uvsX-uvsY interactions in the presynaptic filament has been a matter of some debate. Biochemical data indicate that uvsX and uvsY form an equimolar complex in solution (unpublished results), and in many assays the stimulation of uvsX activities by uvsY appears to saturate at a uvsY/uvsX ratio of ≈ 1 , suggesting that uvsY can interact with uvsX throughout the presynaptic filament (5, 9–11). The *in vivo* ratio of uvsY/uvsX appears to be much less than 1, however (15). This observation, coupled with *in vitro* evidence that uvsY stimulates strand exchange and RDR reactions at low uvsY/uvsX ratios (5, 10), indicates that the physiologically relevant mode of uvsY action likely involves the nucleation of long uvsX-ssDNA filaments from one or a few bound uvsY hexamers as depicted in Fig. 2A. This does not eliminate the possibility that uvsY and uvsX engage in 1:1 interactions locally within a nucleation complex.

Is Presynapsis Coupled to the Nucleolytic Resection of dsDNA Ends?

3' ssDNA tails generated during T4 origin-dependent replication are natural primers for RDR because the presence of homology

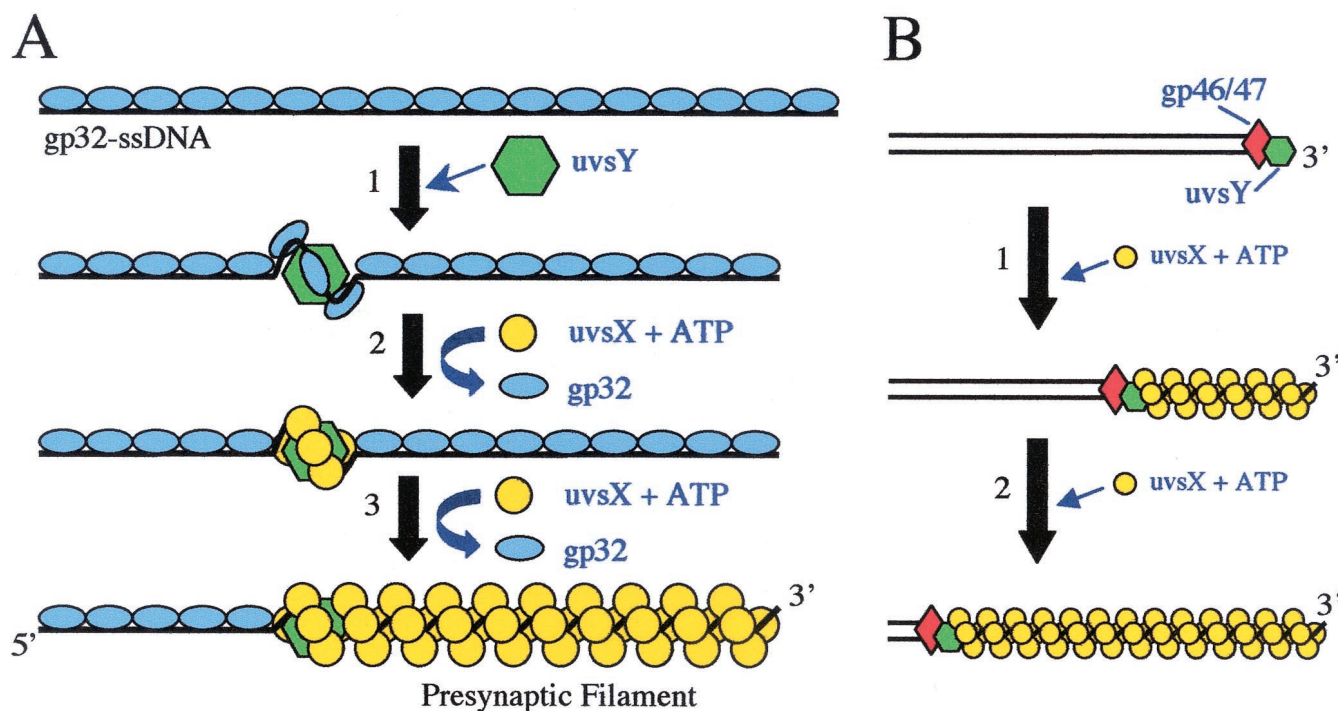


Fig. 2. (A) Biochemical model for uvsY-mediated assembly of the T4 presynaptic filament. Step 1: Hexameric uvsY protein binds to gp32-ssDNA complex and destabilizes gp32-ssDNA interactions. Step 2: UvsX recombinase is recruited to the uvsY-gp32-ssDNA intermediate and locally displaces gp32 to nucleate a filament. Step 3: UvsX-ssDNA filament assembly propagates in the 5' \rightarrow 3' direction while displacing gp32. (B) Hypothetical model for presynapsis coupled to gp46/47-catalyzed resection of a DSB. Step 1: DSB is resected in 5' \rightarrow 3' direction by gp46/47 exonuclease activity, generating a 3' ssDNA tail. Gp46/47 simultaneously recruits uvsY protein, which in turn recruits uvsX. Step 2: Ongoing recruitment of uvsX by gp46/47 + uvsY leads to continuous presynaptic filament formation as the ssDNA tail is exposed by nuclease action, preparing the tail for immediate entry into RDR/double-strand break repair processes.

is guaranteed by the terminal redundancy of T4 DNA (2, 3). Several other mechanisms exist for 3' tail generation, including nucleolytic resection of DNA double-strand breaks (DSBs). It is clear that such breaks can generate primers for T4 RDR, because DSBs induced *in vivo* are repaired by a mechanism that is essentially indistinguishable from RDR (16, 17). Both DSB repair and "normal" RDR processes depend on the T4 gp46 and gp47 proteins. These proteins are proposed components of a multisubunit exonuclease involved both in recombination/replication and degradation of the *E. coli* chromosome after T4 infection (18). Recently, our laboratory overexpressed, purified, and began characterization studies of gp46/47 (details to be published elsewhere). Preliminary results revealed two important properties of gp46/47 germane to this article (Tables 1 and 2): The complex contains a 5' → 3' exonuclease activity, and it interacts specifically with the uvsY protein. The 5' → 3' exonuclease activity makes this enzyme a strong candidate for the resection activity that generates 3' ssDNA-tailed primers for T4 DSB repair and other RDR processes.

The observation of a strong protein-protein interaction between gp46/47 and uvsY raises another intriguing possibility: that nucleolytic resection of DSBs is directly coupled to the assembly of a presynaptic filament on the remaining strand. A hypothetical model for this process is shown in Fig. 2B. Here, as gp46/47 resects a DSB it simultaneously recruits uvsY, which in turn recruits uvsX, so that the expanding 3' ssDNA tail is immediately sequestered in a presynaptic filament without need for a gp32 binding step. This coupling mechanism would ensure a high probability that the resected end would invade a homologous duplex and prime RDR, thus repairing the DSB by a copy-choice mechanism. In summary, in addition to resecting dsDNA ends, by interacting with uvsY gp46/47 may further stimulate RDR by "loading the loader" of the T4 presynaptic filament. This model is reminiscent of one proposed for RecBCD-facilitated loading of RecA protein onto ssDNA generated during RecBCD-catalyzed exonucleolytic processing of dsDNA (19). Further experimentation is needed to test the hypothetical model in Fig. 2B.

Mechanism of DNA Helicase Loading by Gp59

Gp59 stimulates DNA synthesis by the T4 replisome by helping to load the replicative DNA helicase, gp41, at the replication fork (20). The biochemical properties of gp59 include the following (20–27): Gp59 exists in solution and crystallizes as a 26-kDa monomer. The x-ray crystal structure reveals two globular, largely alpha-helical domains separated by a hinge region. The N-terminal domain exhibits structural homology with a family of eukaryotic HMG-I proteins. Gp59 exhibits several DNA binding modes including cooperative, sequence-nonspecific binding to ssDNA, sequence-nonspecific binding to duplex DNA, and structure-specific binding to fork and cruciform DNAs. Gp59 binds specifically to and modulates the enzymatic properties of the gp41 helicase. It also binds specifically and with very high affinity to gp32, forming stable contacts primarily with the acidic, C-terminal domain of the latter (the so-called "A-domain" of gp32). Gp59 is capable of binding to gp41 and gp32 simultaneously, suggesting an adapter function for gp59.

Gp59 is essential for loading gp41 helicase onto ssDNA molecules saturated with cooperatively bound gp32 (20–22). The "target" for helicase loading appears to be a critical cluster of gp32 and gp59 molecules colocalized on ssDNA. Tripartite gp59-gp32-ssDNA complexes have a condensed and beaded appearance in electron micrographs that is quite distinct from the relatively smooth filaments formed by either protein alone on ssDNA (28). It is interesting to speculate that one "bead" structure represents one functional helicase recruitment site. Within the tripartite complex, gp59-gp32 interactions appear to alter the DNA binding properties of both proteins. Gp32-ssDNA

interactions are destabilized in the presence of gp59, suggesting a mechanism for gp59-mediated displacement of gp32 by incoming gp41 (Fig. 3). This model is very similar to the one proposed for the uvsX/uvsY/gp32 presynapsis system (see Fig. 2A). Additional complexity in the helicase loading system is indicated by the fact that binding of the A-domain fragment of gp32 to gp59 weakens the latter's interactions with both ssDNA and fork DNA species (ref. 28; T.W. and S.W.M., unpublished work). Clearly, gp59 and gp32 have a complicated interrelationship that affects helicase assembly. The importance of this issue to the T4 RDR system is addressed below.

In the absence of gp32, gp59 is capable of recruiting the gp41 helicase onto specific DNA structures including forks and cruciforms (26). It is attractive to speculate that gp59 could target helicase assembly directly to a replication fork or a recombination intermediate. The latter could be important for DNA branch migration given that this phase of uvsX/uvsY-initiated recombination may be helicase-dependent under some conditions (see above). In the case of the replication fork, the forked DNA structure itself could provide a nucleation site for the formation of a cooperative cluster of gp59 and gp32 molecules, thereby reconstituting a helicase assembly site directly coupled to a nascent replication fork (Fig. 3). However the significance of structure-specific helicase loading is unclear because it appears that interactions with gp32 may attenuate at least some of gp59's structure-specific DNA binding activities (T.W. and S.W.M., unpublished work), and because gp59-dependent primosome loading is strongly inhibited when the target strand has bound uvsX and uvsY (see below).

Suppression of Gp59-Dependent Primosome Assembly by UvsX/UvsY

Gp59 is essential for RDR *in vivo*. Studies of gp59 activity in the T4 RDR *in vitro* system demonstrated that gp59 is necessary in addition to gp41 helicase and gp61 primase for reconstituting the lagging strand synthesis component of the reaction (J. Barry, M. L. Wong, and B. Alberts, personal communication; reviewed in ref. 2). UvsX protein was shown to inhibit the gp41 helicase, thereby preventing primosome function and lagging strand synthesis (4). Experiments conducted by Jack Barry and Bruce Alberts (personal communication) first revealed that uvsX-ssDNA filament formation interferes with gp41 helicase assembly and primosome function on ssDNA, even in the presence of gp59. Instead, in the presence of uvsX protein, helicase assembly and primosome function require gp32 in addition to gp59. This effect is reproduced in the experiment shown in Table 3, wherein the ability of the T4 primosome (gp41 + gp61 ± gp59) to prime DNA synthesis on ssDNA circles is tested in the presence/absence of bound gp32, uvsX, and/or uvsY. Under the reaction conditions used in Tables 3 and 4, priming on naked ssDNA circles (no gp32, uvsX, or uvsY) occurs readily and is not gp59-dependent, although gp59 stimulates the reaction moderately (ref. 20; unpublished results). However, there is a strong requirement for gp59 to stimulate priming activities on ssDNA saturated with gp32 (Table 3, experiment 1). In contrast, priming activity is completely inhibited when uvsX protein saturates ssDNA in the absence of gp32, and gp59 cannot rescue priming activity under these conditions (Table 3, experiment 2). But when uvsX and gp32 are simultaneously present at ssDNA-saturating concentrations, a minute amount of priming activity is seen in the absence of gp59, and the addition of gp59 strongly stimulates priming (Table 3, experiment 3). This study reproduces the findings of Barry and Alberts and supports their conclusion that gp59 targets helicase and primosome assembly onto patches of gp32 that interrupt uvsX-ssDNA filaments.

We next addressed the question of how uvsY protein affects the priming reaction. When gp32 saturates the ssDNA and no

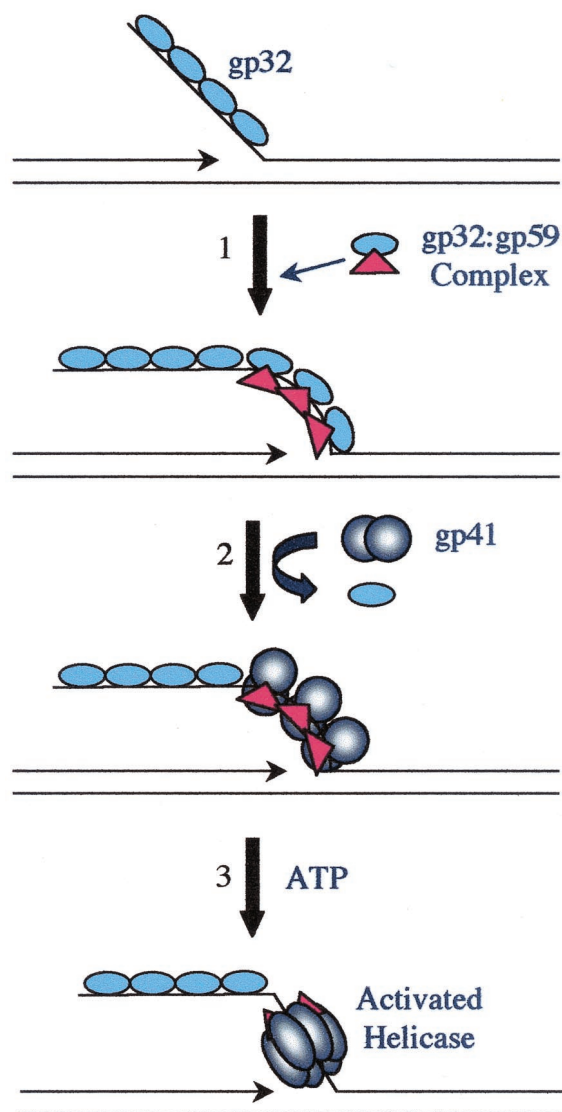


Fig. 3. Biochemical model for gp59-mediated helicase assembly at T4 replication fork. Step 1: Nascent strand-displacing replication fork (DNA polymerase holoenzyme plus gp32). Cluster of gp32-gp59 complexes is incorporated at growing end of gp32 lagging-strand complex. Affinity of gp59 for fork DNA may help nucleate the cluster. Step 2: Gp59 recruits dimers of gp41 helicase to the cluster and promotes displacement of gp32. Step 3: Gp59 stimulates ATP binding by gp41, triggering ring-hexamers formation by the helicase. Gp41-gp59 complex translocates with the replication fork, ready to recruit primase.

UvsX is present, uvsY has little effect on priming activity, and a strong stimulation of the reaction by gp59 is still observed (Table 3, compare experiments 1 and 4). When uvsX protein saturates the ssDNA and gp32 is absent, complete inhibition of priming is observed independent of uvsY or gp59 (Table 3, experiments 2 and 5). But when uvsX and gp32 are simultaneously present at ssDNA-saturating concentrations, the presence of uvsY protein almost completely suppresses the ability of gp59 to rescue priming activity (Table 3, compare experiments 3 and 6). These results suggest that by helping uvsX protein displace gp32 and saturate the ssDNA, uvsY protein effectively precludes the assembly and activity of the T4 primosome. The uvsY concentration used in Table 3 (experiments 4–6) was 1.2 μM , which is 50% saturating with respect to potential ssDNA binding sites (7) and a 4.2-fold molar deficit with respect to uvsX protein. UvsY's suppression of priming activity in the presence of uvsX, gp32,

Table 3. Effects of Gp32, Gp59, UvsX, and UvsY proteins on primosome-initiated DNA synthesis reactions

Expt.	gp32	UvsX	UvsY	DNA synthesis (pmol)	
				– gp59	+ gp59
1	+	–	–	1.8	8.4
2	–	+	–	0.0	0.1
3	+	+	–	0.5	5.1
4	+	–	+	3.2	9.7
5	–	+	+	0.1	0.1
6	+	+	+	0.1	0.4

T4 replication and recombination proteins and M13mp19 ssDNA circles were purified as described (21, 31–34). Assays for *de novo* priming of DNA synthesis on ssDNA circles were carried out as follows: Reactions (15 μl) were carried out at 37°C, and each contained 20 mM Tris-acetate (pH 7.4), 10 mM magnesium acetate, 90 mM potassium acetate, 100 $\mu\text{g}/\text{ml}$ BSA, 0.5 mM DTT, 10 mM creatine phosphate, 10 $\mu\text{g}/\text{ml}$ creatine phosphokinase, 4 $\mu\text{g}/\text{ml}$ gp43, 25 $\mu\text{g}/\text{ml}$ gp44/62, 8 $\mu\text{g}/\text{ml}$ gp45, 5 $\mu\text{g}/\text{ml}$ (80 nM) gp41, 0.5 $\mu\text{g}/\text{ml}$ gp61, 0 or 100 $\mu\text{g}/\text{ml}$ (0 or 2.9 μM) gp32, 0 or 2 $\mu\text{g}/\text{ml}$ (0 or 80 nM) gp59, 0 or 220 $\mu\text{g}/\text{ml}$ (0 or 5 μM) uvsX, 0 or 20 $\mu\text{g}/\text{ml}$ (0 or 1.2 μM) uvsY, 2 mM ATP, 2 mM GTP, 150 μM each UTP, CTP, dATP, dGTP, dCTP, and dTTP, 15 μCi α -[^{32}P]-dTTP, and 10 μM (nucleotides) M13mp19 ssDNA. The presence/absence of variable components is indicated. Each reaction was initiated by the addition of nucleotides and ssDNA. After 10 min reaction time, a 9- μl aliquot was removed and assayed for acid-insoluble [^{32}P] counts as described (4).

and gp59 proteins depends strongly on the concentration of uvsY (Table 4). The lowest concentration tested at which complete inhibition of priming was observed was 1.2 μM uvsY, the concentration used in Table 3. Approximately 50% inhibition of priming is seen at 0.6 μM uvsY, which is only 25% saturating with respect to ssDNA and an 8.4-fold molar deficit with respect to uvsX. These results indicate that the suppression of gp59-dependent priming by uvsX/uvsY does not require saturation of the presynaptic filament with uvsY.

Enzyme Partitioning Is Orchestrated by RMPs

The suppression of gp59-dependent primosome function by uvsX/uvsY (Tables 3 and 4) suggests a mechanism for the strand-specific synthesis of Okazaki fragments observed in the T4 RDR *in vitro* system (see Fig. 1). A model for this reaction based on enzyme partitioning orchestrated by the T4 RMP proteins, uvsY and gp59, is shown in Fig. 4. Here, uvsY helps maintain the saturation of ssDNA 5' of the trailing junction with uvsX protein by promoting the displacement of gp32. This effectively denies gp59 the opportunity to assemble primosome on this strand. Instead, primosome assembly is directed via gp59-gp32 interactions to the displaced strand of the D-loop recombination intermediate, which is destined to become the lagging strand template of a semiconservative replication fork (Fig. 4). Kodadek (29) observed that gp32 promotes uvsX-catalyzed DNA strand exchange reactions by binding to and sequestering the displaced strand of the D loop. Therefore the displaced strand of the D-loop structure that initiates RDR is

Table 4. Effect of UvsY concentration on priming reaction in the presence of Gp32, Gp59, and UvsX

[UvsY], μM	DNA synthesis, pmol
0	8.6
0.3	8.7
0.6	4.1
1.2	0.4
3.1	0.1

Reaction conditions were identical to Table 3, except that each reaction contained 100 $\mu\text{g}/\text{ml}$ (2.9 μM) gp32, 2 $\mu\text{g}/\text{ml}$ (80 nM) gp59, 220 $\mu\text{g}/\text{ml}$ (5 μM) uvsX, and the uvsY concentration varied from 0 to 50 $\mu\text{g}/\text{ml}$ (0–3.1 μM).

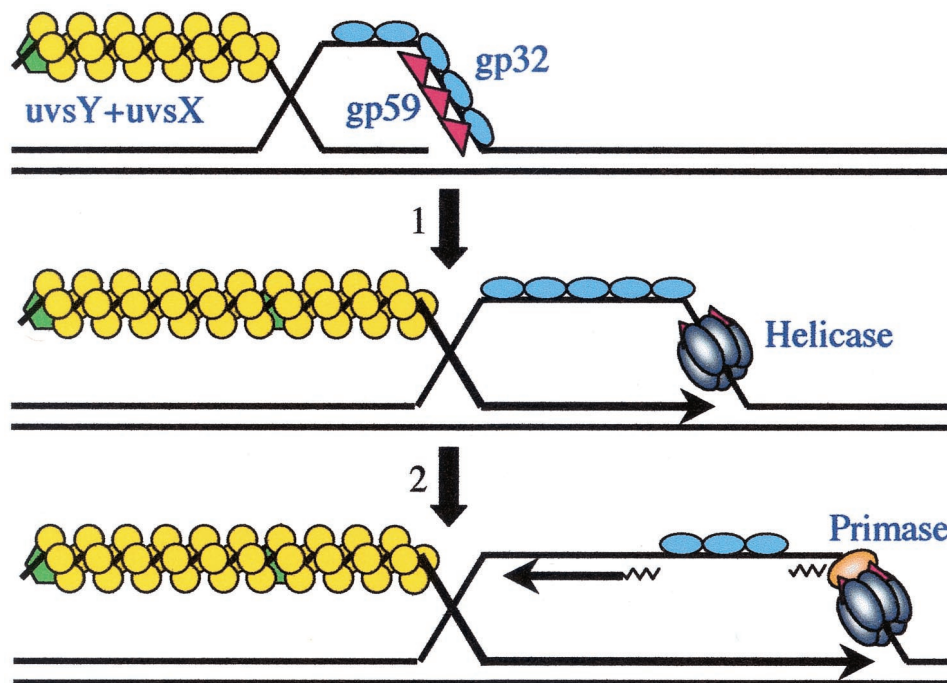


Fig. 4. Enzyme partitioning model for strand-specific priming of Okazaki fragments during T4 recombination-dependent replication. Step 1: Gp32 sequesters the displaced strand of the D loop after *UvsX*-catalyzed invasion of the primer strand. A cluster of gp32-gp59 complexes forms on the displaced strand as shown in Fig. 3. The invading strand ssDNA 5' of the trailing junction remains sequestered by a *UvsY*-stabilized *UvsX*-ssDNA presynaptic filament. Gp41 helicase assembly therefore is directed to the gp32/gp59-enriched D-loop ssDNA and is precluded from the invading strand. Step 2: Recruitment of primase by the gp41 helicase reconstitutes lagging strand synthesis and a normal semiconservative replication fork specifically from within the D-loop bubble.

enriched in bound gp32, and more gp32 molecules will be added to the complex in a 5' → 3' direction as the initial gp32-dependent strand-displacement synthesis reaction takes place. Thus gp59 and gp32 may assemble a helicase loading target on the displaced strand of the D loop via the mechanism shown in Fig. 3, resulting in the recruitment of gp41 helicase to this strand, followed by primase to reconstitute an active primosome (Fig. 4). What keeps *UvsY/UvsX* from assembling onto the displaced D-loop strand and competing with gp59/gp41? An attractive feature of the model in Fig. 2B is that the nuclease-coupling mechanism could be used to restrict filament assembly to DNA ends processed by gp46/47. This restriction combined with the extremely high affinity of gp59 for gp32 protein (27) would help to ensure that assembly of helicase, not presynaptic filament, is targeted to the D loop.

It is also possible that *UvsX/UvsY* interfere with later steps of primosome assembly or function, e.g., recruitment of primase, primer synthesis, or extension of primers by DNA polymerase holoenzyme, and that this interference accounts for some of the strand specificity of primosome function. Also, because Okazaki fragment synthesis on the displaced D-loop strand arrests branch migration and bubble migration synthesis (J. Barry, M. L. Wong, and B. Alberts, personal communication), it appears likely that any helicase acquired by the trailing junction is forced to dissociate once it encounters the lagging strand duplex. These and other questions about our partitioning model (Fig. 4) remain to be addressed experimentally.

The role of *UvsY* protein in helping to enforce the strand specificity of lagging strand synthesis during T4 RDR may provide a functional rationale for the *UvsY* paradox mentioned previously: Why does this protein stimulate the presynapsis and synapsis phases of recombination but inhibit branch migration? We suggest that *UvsY* may have evolved to optimize the initiation of RDR by rapidly promoting the sequestration and strand invasion of 3' ssDNA tails by *UvsX* protein, while effectively stabilizing the resulting D-loop structures from untimely reso-

lution either by *UvsX*-catalyzed branch migration or by the activity of helicases such as gp41. Thus by stabilizing filaments and inhibiting branch migration, *UvsY* may increase the lifetimes of strand invasion products so that the likelihood of initiating RDR increases at the expense of potential antirecombination activities. This strategy makes good sense for T4 replication, because the phage relies heavily on RDR to replicate its genome as well as on recombinational repair pathways such as DSB repair that use RDR mechanisms.

Bubble Migration: A Mechanism for Lesion Bypass?

Some important questions remain about the mechanism of T4 RDR. Is there a biological function for the bubble migration mode of RDR shown in Fig. 1? The observations of J. Barry, M. L. Wong, and B. Alberts (personal communication) indicate that this mode shuts down rapidly once lagging strand synthesis begins. Yet, in the absence of primase, gp41/gp59 are apparently able to promote this reaction. The observations that gp59 can recruit gp41 helicase onto three-stranded junctions and promote branch migration (14, 26) suggest that under some conditions (i.e., a delay in lagging strand synthesis, such as might occur on heavily damaged templates) gp41/gp59 might help bring about a bubble migration reaction. Bubble migration synthesis has been proposed both as a mechanism for DSB repair and for replicative bypass of DNA lesions by a copy-choice mechanism (4). Evidence for the latter reaction occurring in one version of the T4 RDR *in vitro* system is presented in Fig. 5.

An assay for "template switching" of RDR in response to a DNA lesion was designed; the DNA primer and template system is shown in Fig. 5A. Here, priming of RDR by a specific ssDNA oligonucleotide on a damaged template containing a site-specific psoralen adduct would generate a "stall" product of known length when the replication bubble stalls at the adduct. To this system was added a homologous rescue template—a restriction fragment overlapping and homologous to the region surrounding the psoralen adduct in the damaged

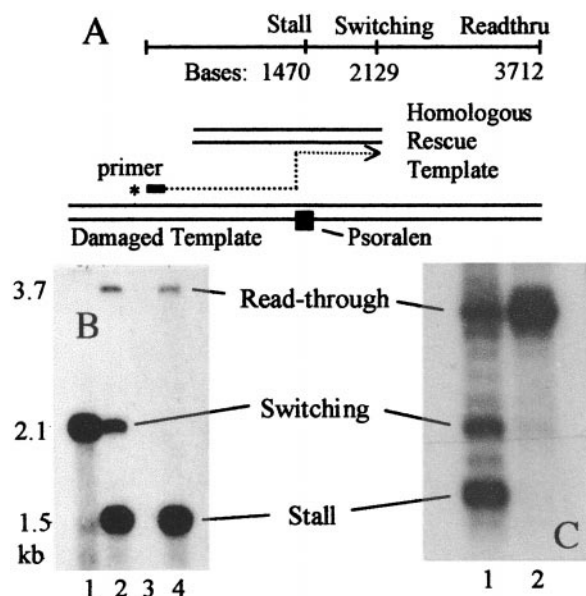


Fig. 5. Template switching assay for lesion bypass under conditions supporting bubble migration synthesis by the T4 RDR *in vitro* system. (A) DNA primer and template design for template switching assay. Damaged template contains a site-specific psoralen monoadduct on the (–) strand at position 6276 in M13mp19 dsDNA. Supercoiled, psoralenated DNA was synthesized as described (35), then linearized with *Sna*BI. Homologous rescue template is the short *Bal*–*Bgl*II restriction fragment of M13mp19 dsDNA, which overlaps the psoralenated site in the damaged template. The ssDNA primer is a 5′-[³²P]-100-mer complementary to the (–) strand of M13mp19 dsDNA at positions 4806–4905. This primer initiates RDR on the damaged template but not on the homologous rescue template. The dotted arrow denotes the replicative path needed to generate the switching product (see text). (B) Template switching assay and controls. Reactions (15 μ l) at 37°C contained 20 mM Tris-acetate, pH 7.4, 10 mM magnesium acetate, 90 mM potassium acetate, 0.5 mM DTT, 50 μ g/ml BSA, 10 μ g/ml creatine phosphokinase, 10 mM creatine phosphate, 0.25 mM spermine, 0.15 mM spermidine, 3.8 μ g/ml gp43, 25 μ g/ml gp44/62, 8 μ g/ml gp45, 85 μ g/ml gp32, 4 μ g/ml dda, 18 μ g/ml gp41, 2 μ g/ml gp59, 20 μ g/ml uvsX, 5 μ g/ml uvsY, 2 mM ATP, 1.75 mM GTP, 200 μ M each dATP, dGTP, dCTP, and dTTP, 2 μ M 5′-[³²P]-100-mer, 10 μ M damaged template, and 10 μ M homologous rescue template. (All DNA concentrations in nucleotides.) Some control reactions contained 10 μ M heterologous pBR322 restriction fragments in place of homologous templates. Each reaction was initiated by the addition of DNAs and nucleotides, incubated for 10 min, then analyzed by alkaline agarose gel electrophoresis and autoradiography as described (4). Lane 1: Size marker for position of stall product. Lane 2: Complete template switching reaction containing primer, damaged template, and homologous rescue template. Lane 3: Control reaction containing *Xmn*I-digested pBR322 dsDNA in place of damaged template. Lane 4: Control reaction containing *Xmn*I-digested pBR322 dsDNA in place of homologous rescue template. (C) Lesion dependence of template switching. Lane 1: Complete reaction identical to lane 2 of B, except that a longer ssDNA primer was used (2,527-bp *Hae*III fragment of M13 ssDNA), and DNA synthesis products were visualized by incorporation of α -[³²P]-dTTP. Lane 2: Same as lane 1 except that the damaged template lacks psoralen.

template. The chosen primer cannot initiate RDR on the homologous rescue template directly. But if RDR primed on the damaged template could switch templates after stalling at the lesion, it should generate a longer “switching” product of discrete length, caused by run-off synthesis on the homologous rescue template. Results are shown in Fig. 5B. In a complete

reaction containing both homologous templates and primer, and performed under conditions that support bubble migration synthesis (but not semiconservative synthesis) by the T4 RDR *in vitro* system, discrete bands appear at both the stall and switching positions (Fig. 5B, lane 2). Therefore template switching works under these conditions. A faint third band higher on the gel represents “read-through” synthesis, due either to translesion synthesis by polymerase or the loss of adduct from a fraction of the damaged templates. The control reaction in Fig. 5B, lane 3 shows that no stall, switching, or read-through bands occur when a pBR322 template is substituted for the damaged template, consistent with the inability of the primer molecule to prime RDR on a heterologous template. The control reaction in Fig. 5B, lane 4 shows that no switching product, or anything resembling a switching product, occurs when a pBR322 fragment of similar length is substituted for the homologous rescue template. Other results prove that template switching is uvsX-dependent (data not shown). Therefore homologous recombination is a requirement for template switching. The experiment in Fig. 5C demonstrates that the template switching reaction strongly depends on the presence of the psoralen adduct on the damaged template. Therefore polymerase stalling at a lesion in the template appears to trigger template switching. However, we noted that under some conditions there can be a relatively high occurrence of template switching that is homology-dependent but damage-independent (data not shown), suggesting that other factors such as stalling of polymerase at DNA secondary structure or at specific sequences in the template also may trigger template switching. Also, template promiscuity may be a general feature of bubble migration synthesis because branch migration may occasionally overtake the replication fork and displace the 3′ end of the daughter strand (4).

The results in Fig. 5 appear to support the proposal by Formosa and Alberts (4) that bubble migration synthesis could provide a mechanism for displacing the 3′ end of a lesion-stalled daughter strand, via branch migration from the trailing edge of the bubble. The liberated ssDNA 3′ end could then serve as a primer for a new round of RDR on a homologous but undamaged template, effectively bypassing the lesion by an error-free, copy-choice mechanism. Conceivably, this mechanism could play a role in T4 recombination repair pathways such as multiplicity reactivation (30). To date, efforts to observe lesion bypass of this type in a semiconservative RDR reaction have been unsuccessful. The inability of the semiconservative system to support DNA branch migration into the lagging strand duplex appears to be the problem. Perhaps further research will turn up new enzyme activities that promote this reaction, or perhaps other processes such as DSB repair will turn out to be a more general repair mechanism for stalled replication forks of all varieties.

We gratefully acknowledge Dr. Bruce Alberts for his support, mentorship, and intellectual creativity on this and many other projects in T4 replication and recombination that we have been privileged to work on. This work was supported by National Institutes of Health Grant R01 GM48847 and American Cancer Society Research Grant RPG-94-036-04-GMC. Lesion bypass experiments were conducted in the laboratory of Dr. Alberts and were funded by an American Cancer Society, California Division Inc., Senior Postdoctoral Fellowship (to S.W.M.).

- Carles-Kinch, K., George, J. W. & Kreuzer, K. N. (1997) *EMBO J.* **16**, 4142–4151.
- Kreuzer, K. N. & Morrical, S. W. (1994) in *Molecular Biology of Bacteriophage T4*, ed. Karam, J. D. (Am. Soc. Microbiol., Washington, DC), pp. 28–42.
- Kreuzer, K. N. (2000) *Trends Biochem. Sci.* **25**, 165–173.
- Formosa, T. & Alberts, B. M. (1986) *Cell* **47**, 793–806.
- Morrill, S. W. & Alberts, B. M. (1990) *J. Biol. Chem.* **265**, 15096–15103.

- Beernink, H. T. H. & Morrical, S. W. (1998) *Biochemistry* **37**, 5673–5681.
- Sweezy, M. A. & Morrical, S. W. (1997) *J. Mol. Biol.* **267**, 927–938.
- Yassa, D. S., Chou, K. M. & Morrical, S. W. (1997) *Biochimie* **79**, 275–285.
- Kodadek, T., Gan, D.-C. & Stemke-Hale, K. (1989) *J. Biol. Chem.* **264**, 16451–16457.
- Yonesaki, T. & Minagawa, T. (1989) *J. Biol. Chem.* **264**, 7814–7820.
- Harris, L. D. & Griffith, J. D. (1989) *J. Mol. Biol.* **206**, 19–28.

12. Sweezy, M. A. & Morrical, S. W. (1999) *Biochemistry* **38**, 936–944.
13. Ando, R. A. & Morrical, S. W. (1998) *J. Mol. Biol.* **283**, 785–796.
14. Salinas, F. & Kodadek, T. (1995) *Cell* **82**, 111–119.
15. Cowan, J., D'Acci, K., Guttman, B. & Kutter, E. (1994) in *Molecular Biology of Bacteriophage T4*, ed. Karam, J. D. (Am. Soc. Microbiol., Washington, DC), pp. 520–527.
16. George, J. W. & Kreuzer, K. N. (1996) *Genetics* **143**, 1507–1520.
17. Mueller, J. E., Clyman, J., Huang, Y. J., Parker, M. M. & Belfort, M. (1996) *Genes Dev.* **10**, 351–364.
18. Nicholson, C. & Weiberg, J. S. (1981) *J. Virol.* **40**, 65–77.
19. Arnold, D. A. & Kowalczykowski, S. C. (2000) *J. Biol. Chem.* **275**, 12261–12265.
20. Barry, J. E. & Alberts, B. M. (1994) *J. Biol. Chem.* **269**, 33049–33062.
21. Morrical, S. W., Beernink, H. T. H., Dash, A. & Hempstead, K. (1996) *J. Biol. Chem.* **271**, 20198–20207.
22. Morrical, S. W., Hempstead, K. & Morrical, M. D. (1994) *J. Biol. Chem.* **269**, 33069–33081.
23. Yonesaki, T. (1994) *J. Biol. Chem.* **269**, 1284–1289.
24. Lefebvre, S. L. & Morrical, S. W. (1997) *J. Mol. Biol.* **272**, 312–326.
25. Mueser, T. C., Jones, C. E., Nossal, N. G. & Hyde, C. C. (2000) *J. Mol. Biol.* **296**, 597–612.
26. Jones, C. E., Mueser, T. C. & Nossal, N. G. (2000) *J. Biol. Chem.* **275**, 27145–27154.
27. Xu, H., Wang, Y., Bleuit, J. S. & Morrical, S. W. (2001) *Biochemistry*, **40**, in press.
28. Lefebvre, S. D., Wong, M. L. & Morrical, S. W. (1999) *J. Biol. Chem.* **274**, 22830–22838.
29. Kodadek, T. (1990) *J. Biol. Chem.* **265**, 20966–20969.
30. Kreuzer, K. N. & Drake, J. W. (1994) in *Molecular Biology of Bacteriophage T4*, ed. Karam, J. D. (Am. Soc. Microbiol., Washington, DC), pp. 89–97.
31. Burke, R. L., Munn, M., Barry, J. & Alberts, B. M. (1985) *J. Biol. Chem.* **260**, 1711–1722.
32. Morris, C. F., Hama-Inaba, H., Mace, D., Sinha, N. K. & Alberts, B. (1979) *J. Biol. Chem.* **254**, 6787–6796.
33. Spacciapoli, P. & Nossal, N. G. (1994) *J. Biol. Chem.* **269**, 447–455.
34. Miller, H. (1987) *Methods Enzymol.* **152**, 145–170.
35. Kodadek, T. & Gamper, H. (1988) *Biochemistry* **27**, 3210–3215.